Electronic Supplementary Material (ESI) for Journal of Materials Chemistry A.

Supporting Information

Efficient Heterojunction Constructed by Wide-Bandgap and Narrow-Bandgap Small Molecules Enables Dual-Band Absorption Transparent Photovoltaics

Ruiqian Meng[1,2,3‡], Ze Qiao[1,2‡], Qianqing Jiang[1,2], Dianyi Liu[1,2,3]*

[1] Key Laboratory of 3D Micro/nano Fabrication and Characterization of Zhejiang Province, School of Engineering, Westlake University, Hangzhou, Zhejiang 310030, China.

[2] Institute of Advanced Technology, Westlake Institute for Advanced Study, Hangzhou, Zhejiang 310024, China.

[3] Zhejiang University, Hangzhou, Zhejiang 310027, China.

a

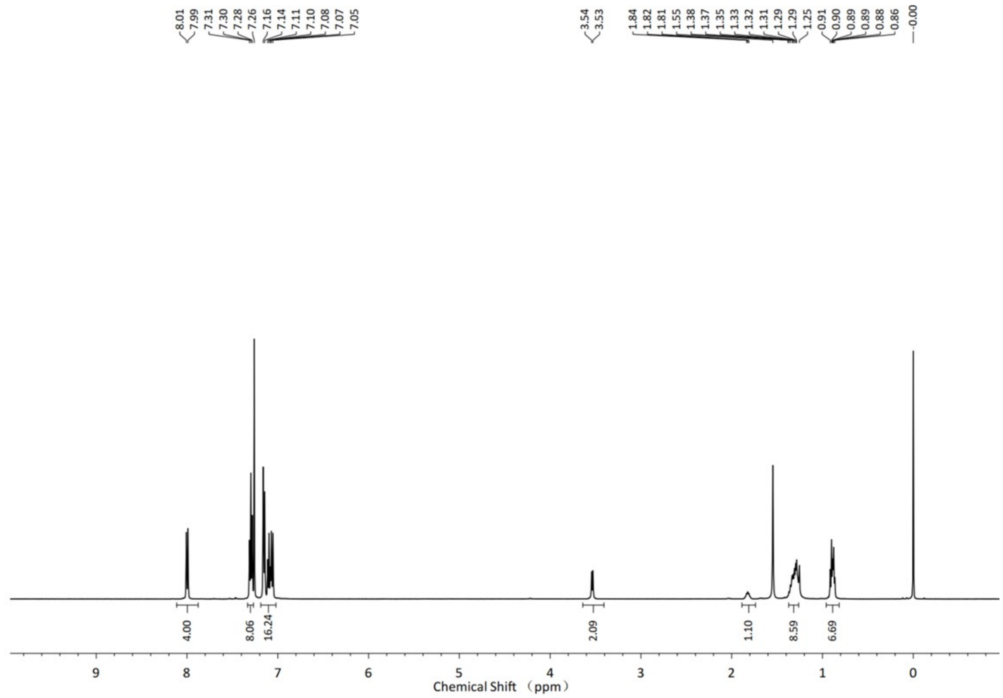

[1]H NMR spectrum of TPD-2TPA ($CDCl_3$,500 MHz)

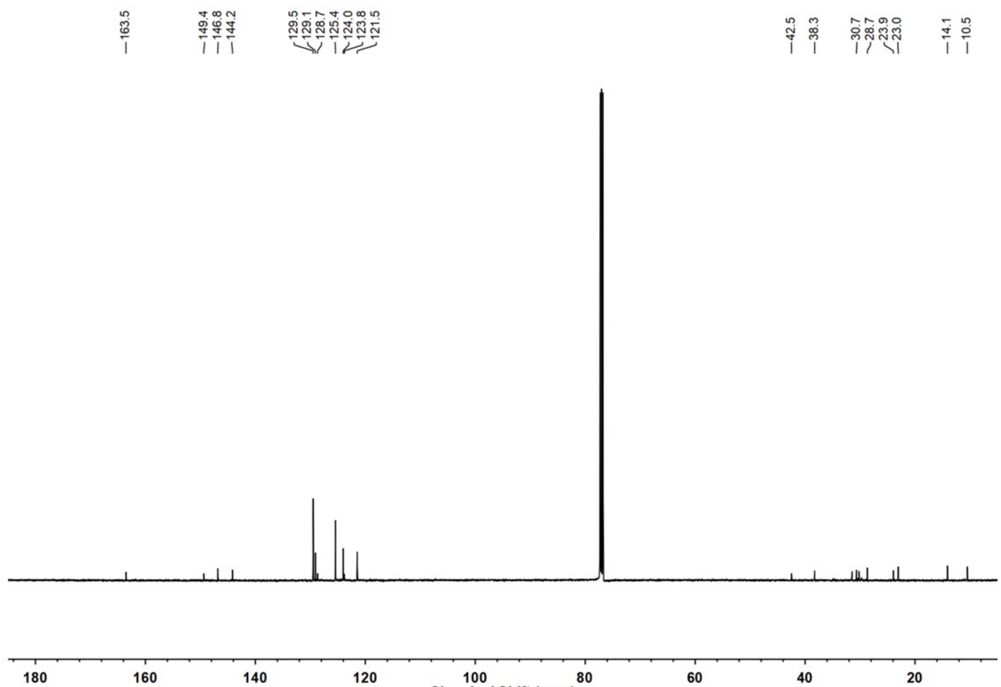

[13]C NMR spectrum of TPD-2TPA ($CDCl_3$,125 MHz)

b

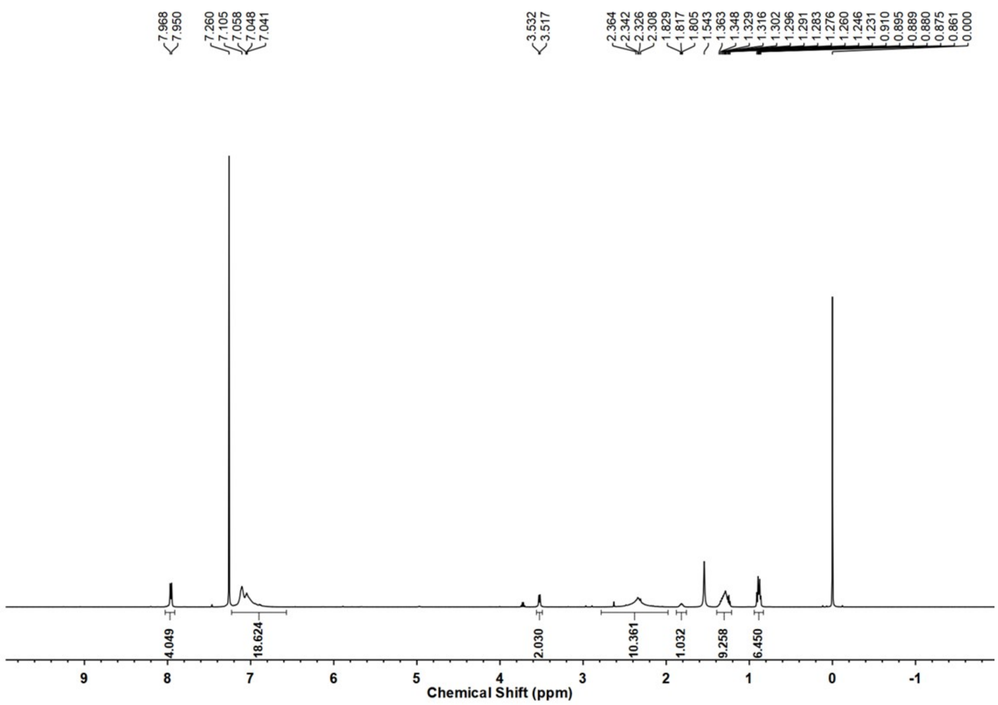

^{1}H NMR spectrum of TPD-2TPA-4Me ($CDCl_3$,500 MHz)

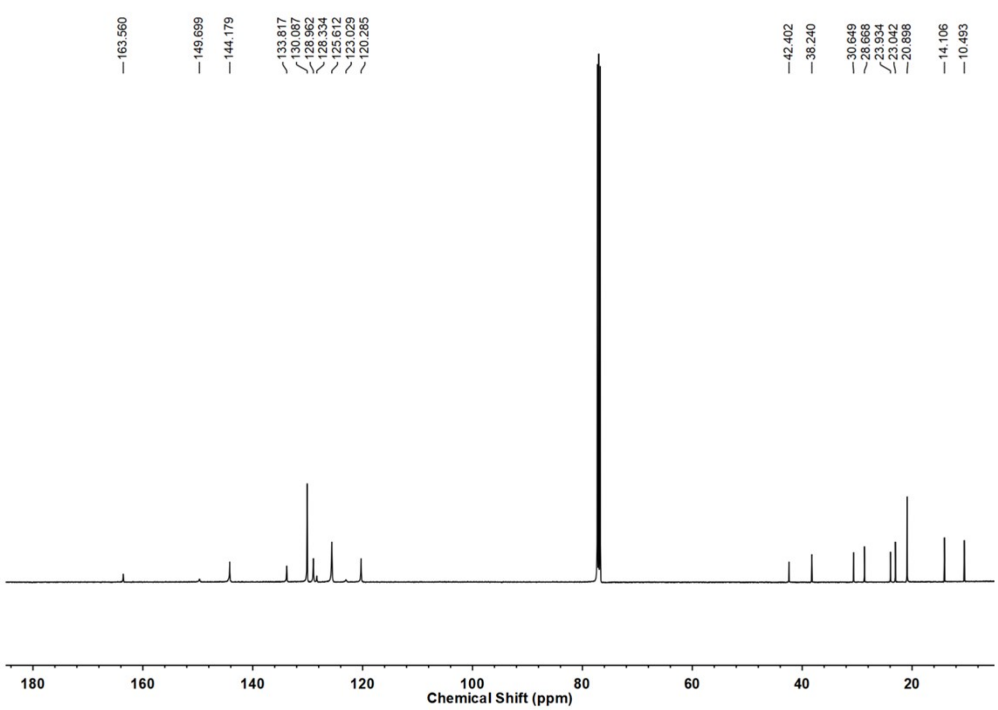

^{13}C NMR spectrum of TPD-2TPA-4Me ($CDCl_3$,125 MHz) c

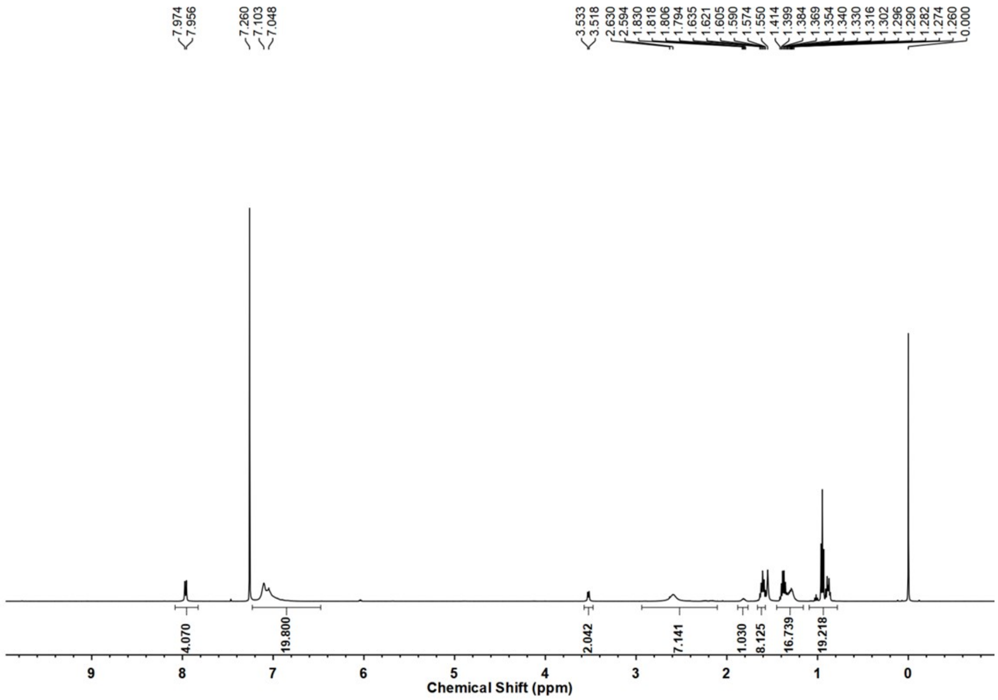

^{1}H NMR spectrum of TPD-2TPA-4Bu ($CDCl_3$, 500 MHz)

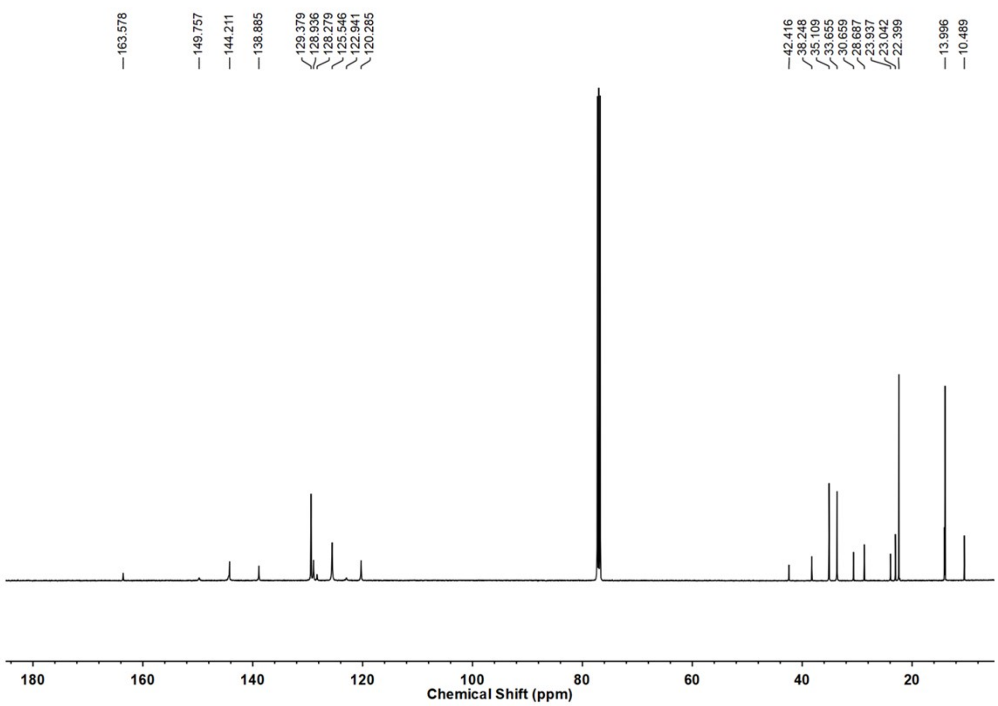

^{13}C NMR spectrum of TPD-2TPA-4Bu ($CDCl_3$, 125 MHz) d

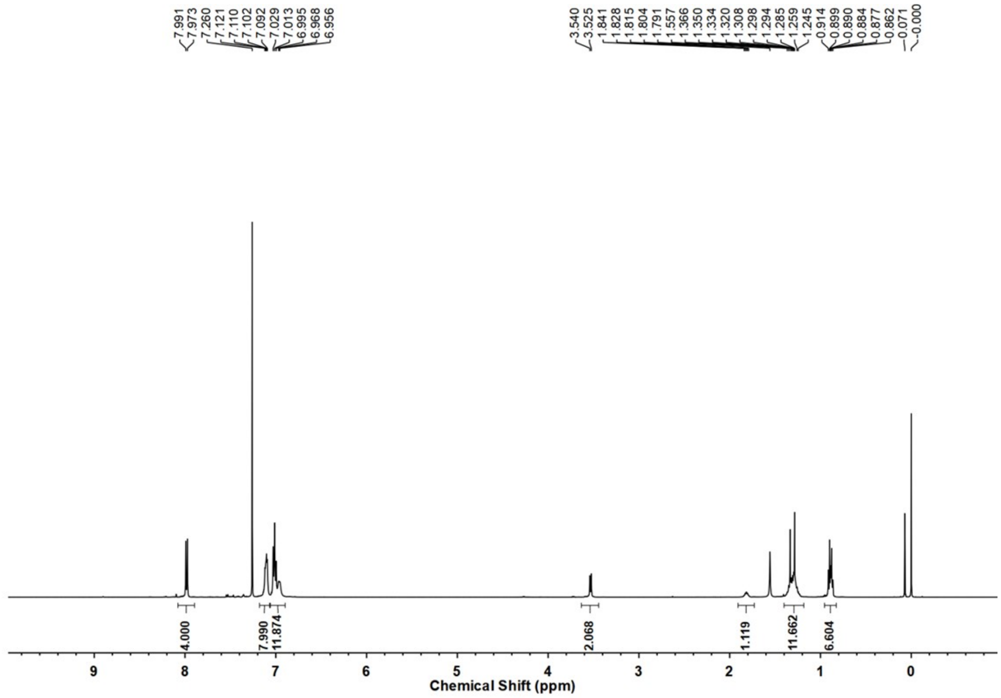

^{1}H NMR spectrum of TPD-2TPA-4F ($CDCl_3$,500 MHz)

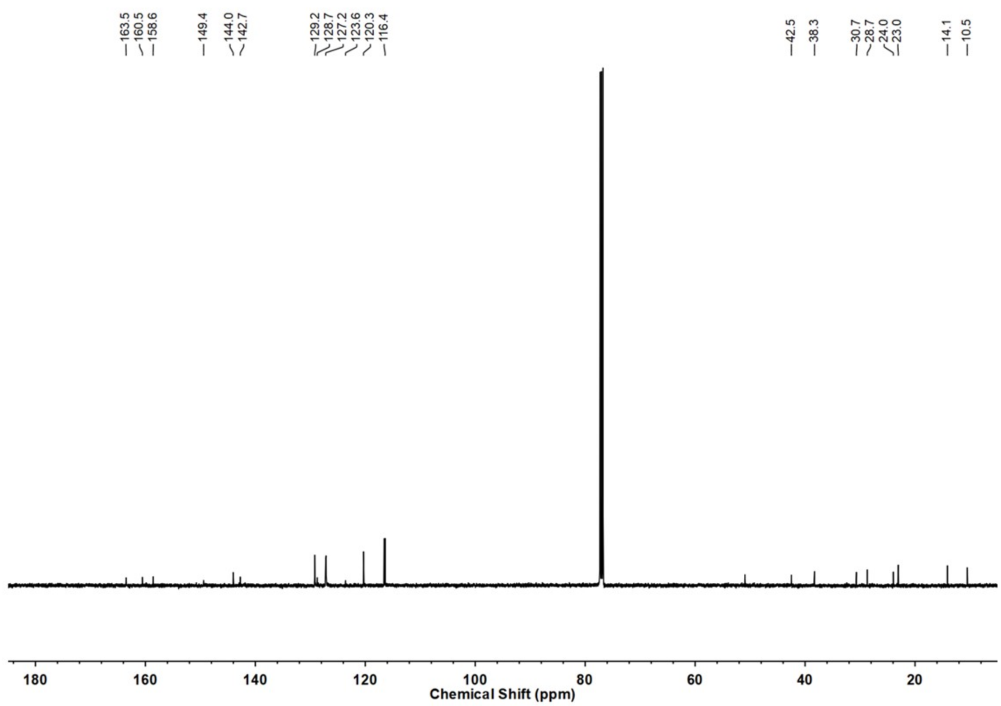

^{13}C NMR spectrum of TPD-2TPA-4F ($CDCl_3$,125 MHz)

Figure S1. NMR spectra of the TPD-2TPA (a), TPD-2TPA-4Me (b), TPD-2TPA-4Bu (c) and TPD-2TPA-4F (d) in $CDCl_3$.

a

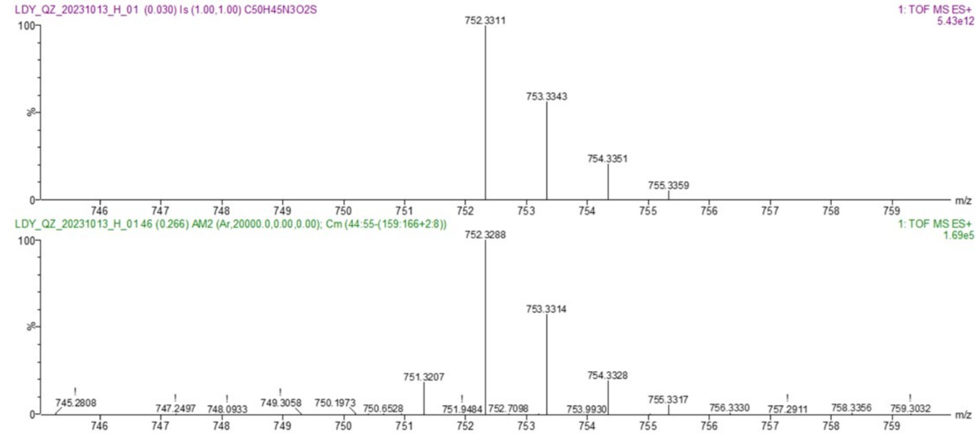

LDY_QZ_20231013_H_01 (0.030) Is (1.00,1.00) C50H45N3O2S
1: TOF MS ES+
5.43e12
752.3311
753.3343
754.3351
755.3359
m/z
LDY_QZ_20231013_H_01 46 (0.266) AM2 (Ar,20000.0,0.00,0.00); Cm (44:55-(159:166+2:8))
1: TOF MS ES+
1.69e5
752.3288
753.3314
751.3207
754.3328
745.2808
747.2497
748.0933
749.3058
750.1973
750.6528
751.9484
752.7098
753.9930
755.3317
756.3330
757.2911
758.3356
759.3032

b

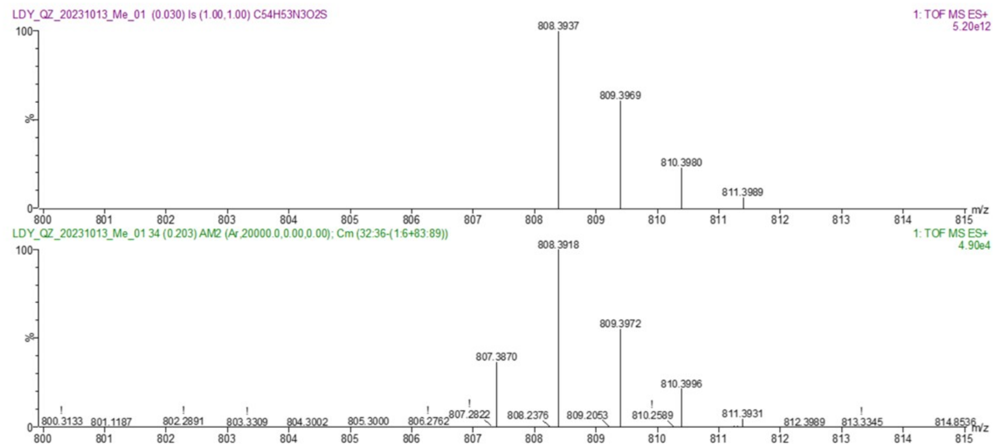

LDY_QZ_20231013_Me_01 (0.030) Is (1.00,1.00) C54H53N3O2S
1: TOF MS ES+
5.20e12
808.3937
809.3969
810.3980
811.3989
m/z
LDY_QZ_20231013_Me_01 34 (0.203) AM2 (Ar,20000.0,0.00,0.00); Cm (32:36-(1:6+83:89))
1: TOF MS ES+
4.90e4
808.3918
809.3972
807.3870
810.3996
800.3133
801.1187
802.2891
803.3309
804.3002
805.3000
806.2762
807.2822
808.2376
809.2053
810.2589
811.3931
812.3989
813.3345
814.8536

c

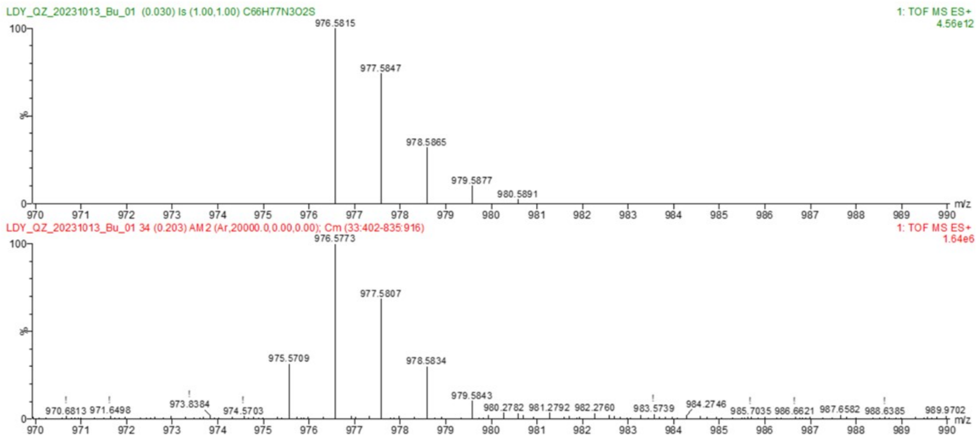

d

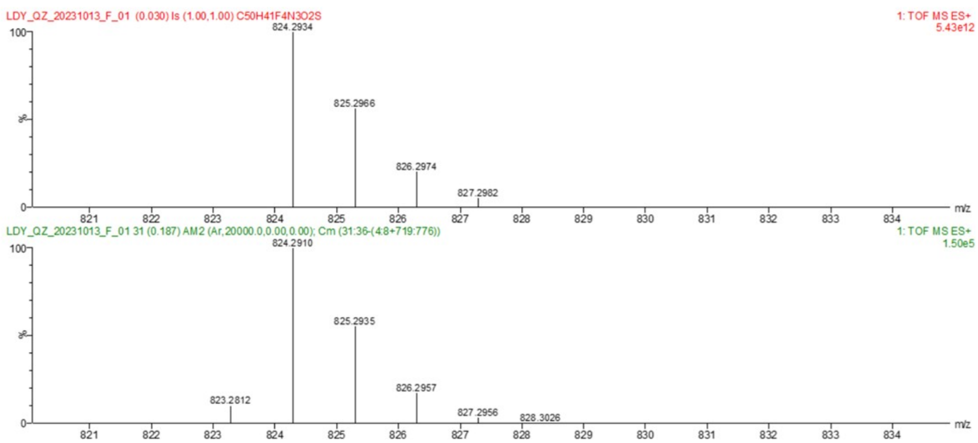

Figure S2. HR-MS (ESI) spectra of the TPD-2TPA (a), TPD-2TPA-4Me (b), TPD-2TPA-4Bu (c) and TPD-2TPA-4F (d).

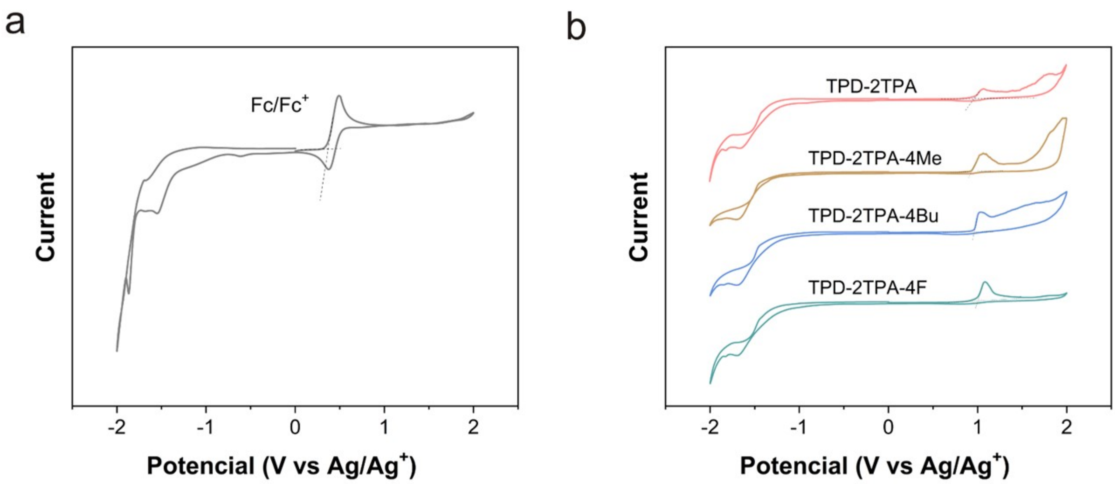

Figure S3. Cyclic voltammograms (CV) (20 mV s^{-1}) of TPD-2TPA-4X (Ag/AgCl as reference electrode).

Table S1. HOMO/LUMO energies related data of TPD-2TPA-4X.

Sample	E_{ox} (eV)	E_{HOMO} (eV)	E_g^{opt} (eV)	E_{LUMO} (eV)
TPD-2TPA	0.98	-5.41	2.48	-2.93
TPD-2TPA-4Me	0.93	-5.36	2.44	-2.92
TPD-2TPA-4Bu	0.94	-5.37	2.43	-2.94
TPD-2TPA-4F	1.00	-5.43	2.51	-2.92

Table S2. Opaque device performances with various SVA durations for active layers.

SVA	Temperature	V_{OC} (V)	J_{SC} /J_{EQE} (mA·cm^{-2})	FF (%)	PCE (%)
0 s	R.T.	0.850	8.72/7.77	38.0	2.82
10 s	R.T.	0.840	11.5/10.8	41.8	4.04
30 s	R.T.	0.815	17.2/17.8	44.2	6.20
1 min	R.T.	0.813	17.4/17.0	44.4	6.29
2 min	R.T.	0.822	14.6/14.2	43.4	5.19

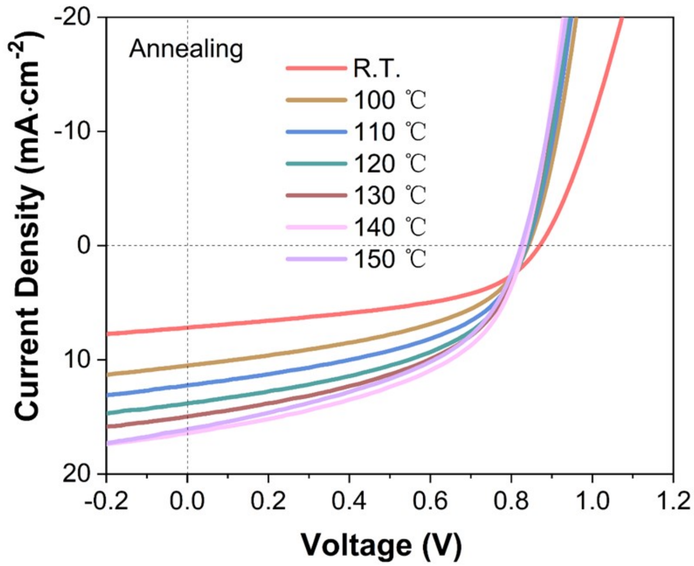

Figure S4. *J-V* curves of opaque devices with different annealing temperatures for active layers.

Table S3. Opaque device performances with different annealing temperatures for active layers.

Anneal	V_{OC} (V)	J_{SC} (mA·cm^{-2})	FF (%)	PCE (%)
R.T.	0.869	7.18	48.4	3.02
100 °C	0.841	10.5	46.7	4.12
110 °C	0.837	12.2	47.8	4.89
120 °C	0.836	13.8	48.5	5.59
130 °C	0.831	14.9	48.0	5.96
140 °C	0.832	16.4	48.1	6.56
150 °C	0.823	16.1	46.1	6.10

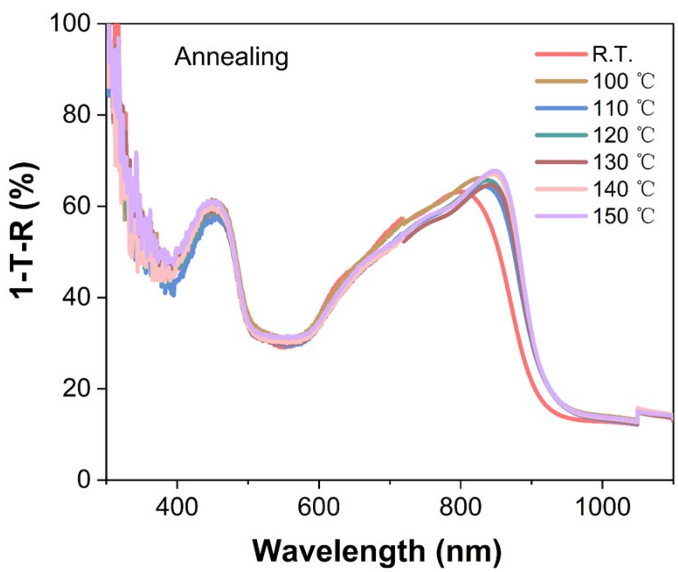

Figure S5. 1-T-R curves of active layers with different annealing temperatures.

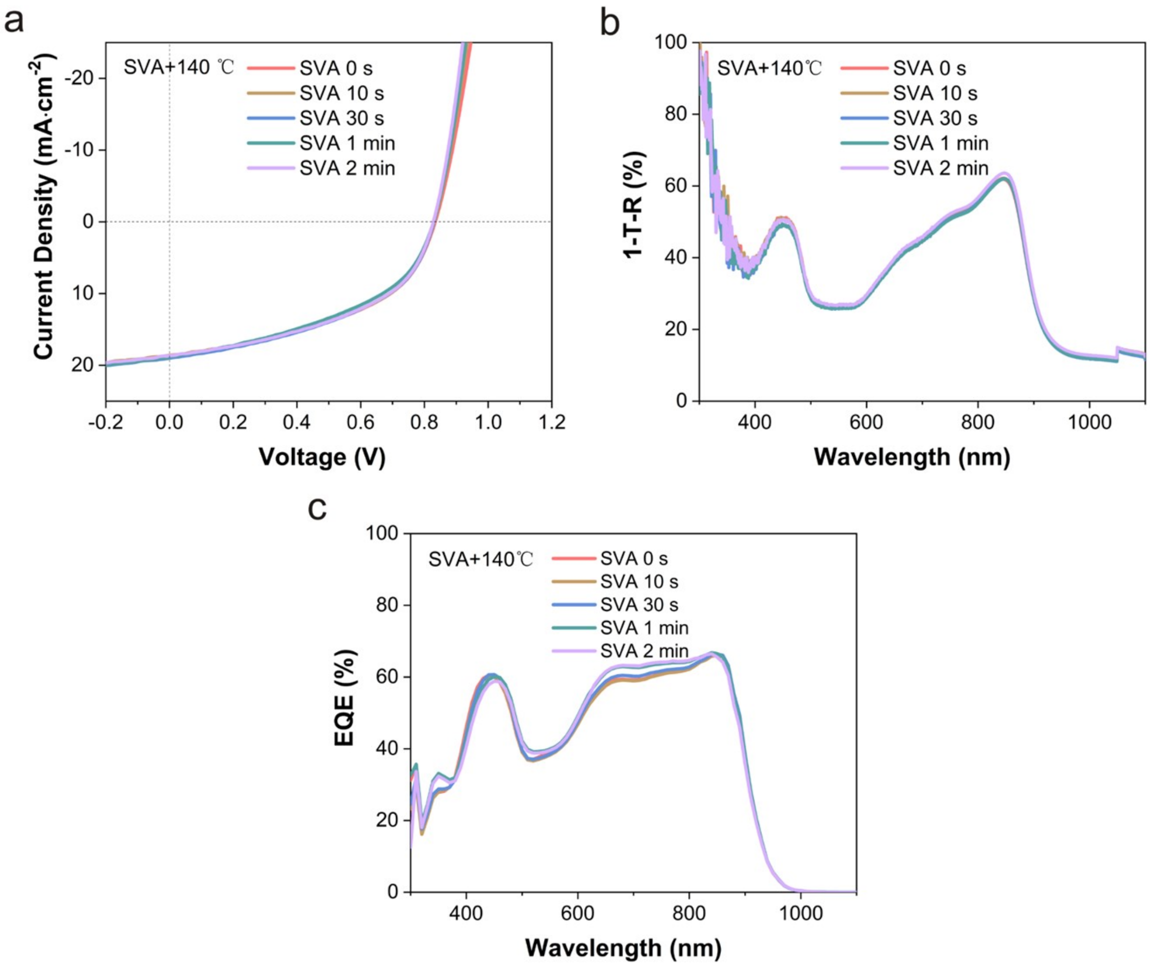

Figure S6. Opaque device performances with various SVA durations and thermal annealing. (a) *J-V* curves of devices. (b) 1-T-R spectra of related films. (c) External quantum efficiency curves of devices.

Table S4. Device performances with SVA and thermal annealing for active layers.

SVA	Temperature	V_{OC} (V)	J_{SC} /J_{EQE} (mA·cm^{-2})	FF (%)	PCE (%)
0 s	140 °C	0.833	18.7/18.5	47.2	7.34
10 s	140 °C	0.830	18.6/18.4	47.5	7.31
30 s	140 °C	0.828	18.9/18.7	46.5	7.30
1 min	140 °C	0.827	18.8/19.1	44.8	6.96
2 min	140 °C	0.827	18.6/18.9	47.3	7.28

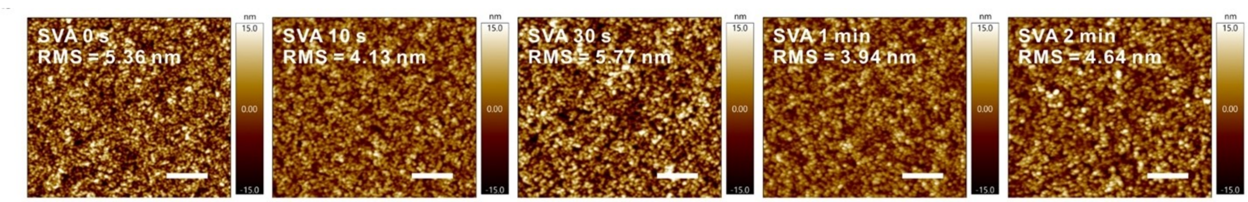

Figure S7. AFM images of TPD-2TPA:Y6 films with various SVA durations and thermal annealing (The scale bar is 1 μm).

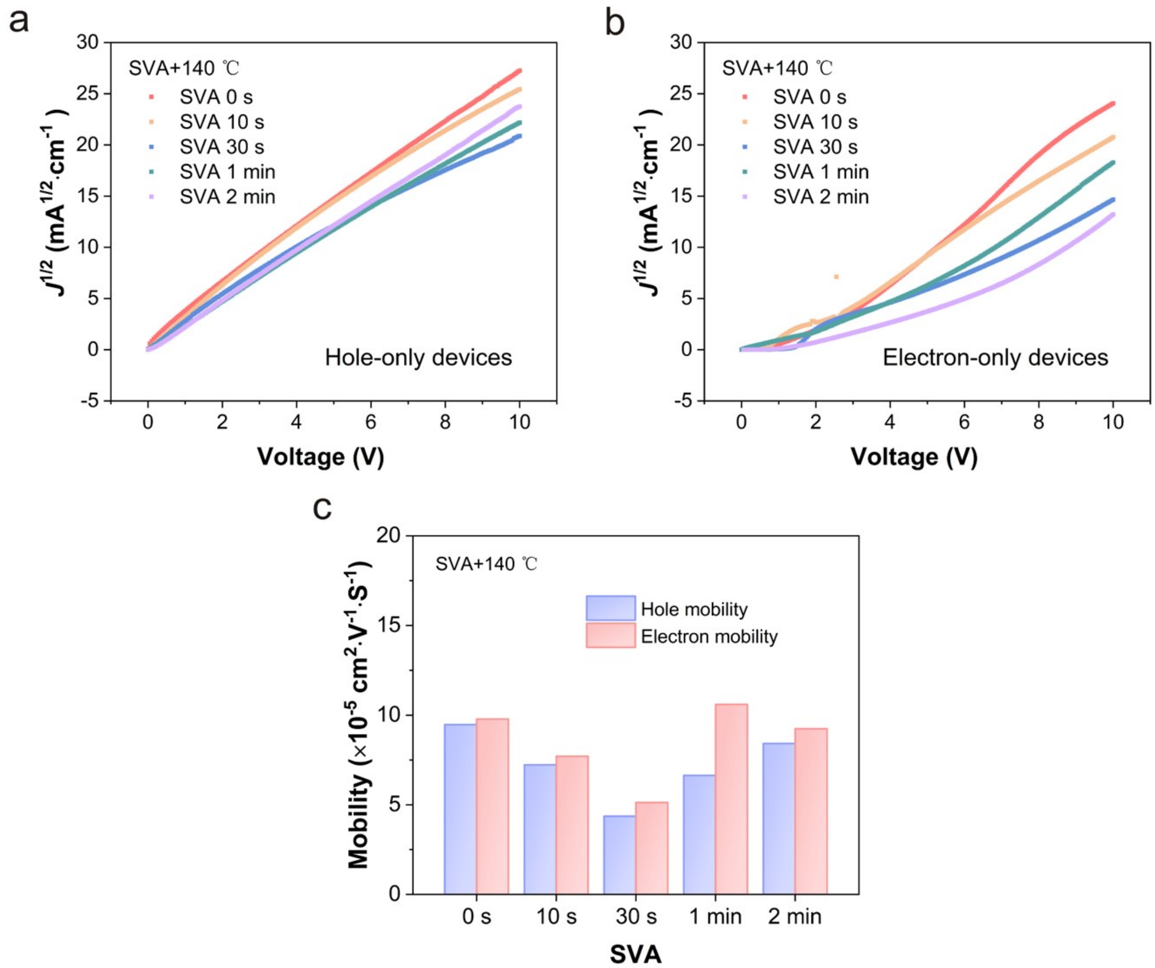

Figure S8. Opaque device performances with various SVA durations and thermal annealing. The *J*–*V* characteristics of hole-only devices (a) and electron-only devices (b). (c) Carrier mobilities acquired from single carrier devices.

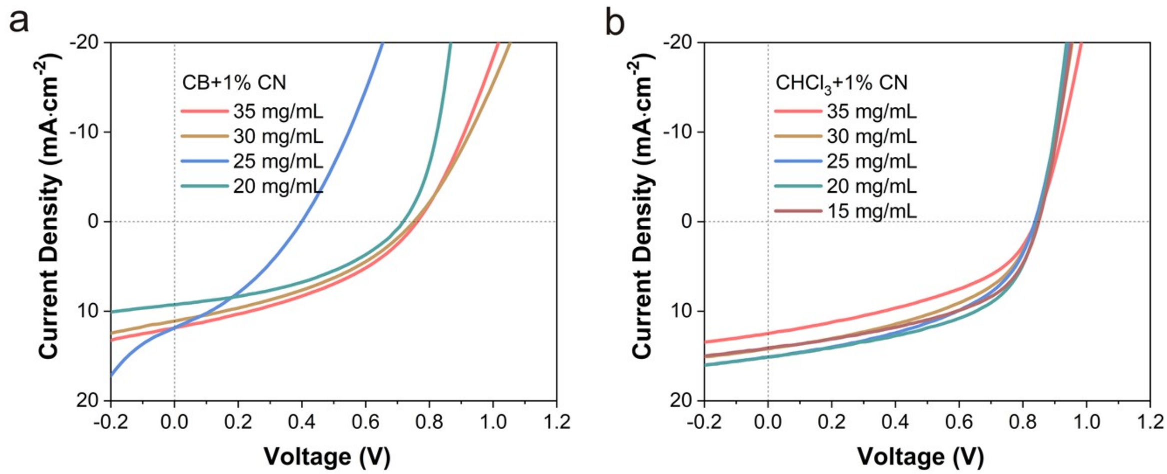

Figure S9. *J-V* curves of devices with different solvents and total concentration for active layers.

Table S5. Device performances with different solvents and total concentrations for active layers.

Solvent	Concentration	V_{OC} (V)	J_{SC} (mA·cm^{-2})	FF (%)	PCE (%)
CB	35 mg/mL	0.760	11.8	38.7	3.48
	30 mg/mL	0.749	11.1	38.0	3.16
	25 mg/mL	0.399	11.9	34.5	1.63
	20 mg/mL	0.716	9.26	41.9	2.78
$CHCl_3$	35 mg/mL	0.839	12.5	43.1	4.51
	30 mg/mL	0.838	14.2	45.8	5.44
	25 mg/mL	0.836	15.1	47.1	5.94
	20 mg/mL	0.845	15.1	51.1	6.53
	15 mg/mL	0.848	14.1	50.1	6.00

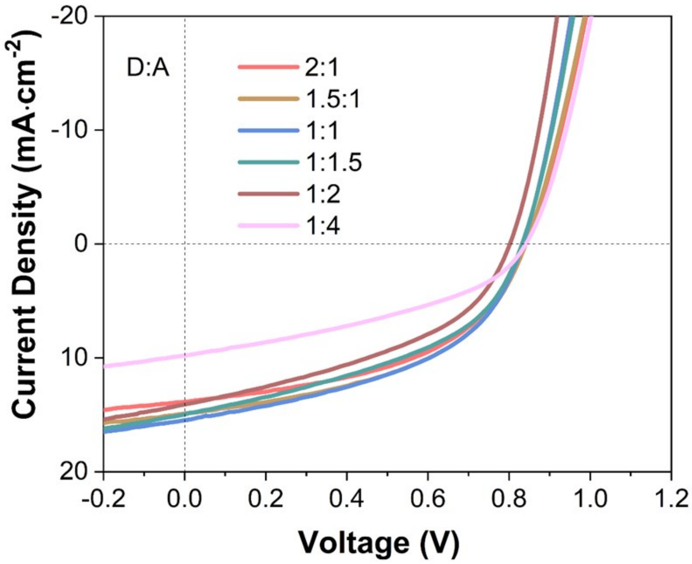

Figure S10. *J-V* curves of devices with different D-A ratios for active layers.

Table S6. Device performances with different D-A ratios for active layers.

D:A	V_{OC} (V)	J_{SC} (mA·cm^{-2})	FF (%)	PCE (%)
2:1	0.839	13.8	48.9	5.67
1.5:1	0.840	14.9	48.3	6.03
1:1	0.832	15.4	46.9	6.03
1:1.5	0.830	14.9	43.9	5.44
1:2	0.800	14.1	42.5	4.79
1:4	0.839	9.78	39.3	3.22

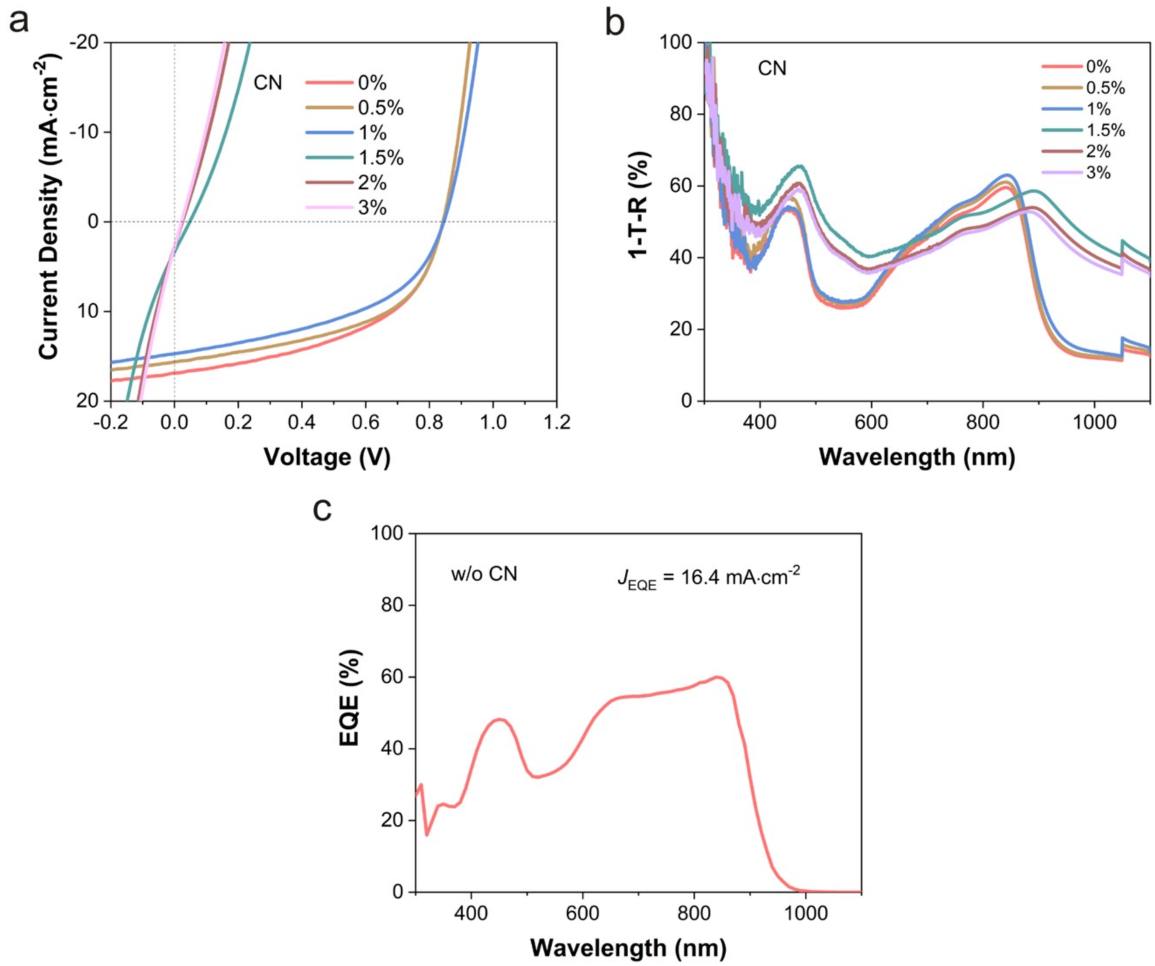

Figure S11. *J*-*V* (a) and 1-T-R (b) curves of devices with different amounts of chloronaphthalene (CN) additive in active layers. (c) EQE curve of the device without CN.

Table S7. Device performances with different amounts of CN additive in active layers.

CN	V_{OC} (V)	J_{SC} (mA·cm^{-2})	FF (%)	PCE (%)
0%	0.842	16.9	49.6	7.04
0.5%	0.842	15.6	51.5	6.77
1%	0.844	14.7	46.8	5.80
1.5%	0.0478	3.34	25.0	0.0400
2%	0.0248	2.76	NaN	NaN
3%	0.0220	2.80	NaN	NaN

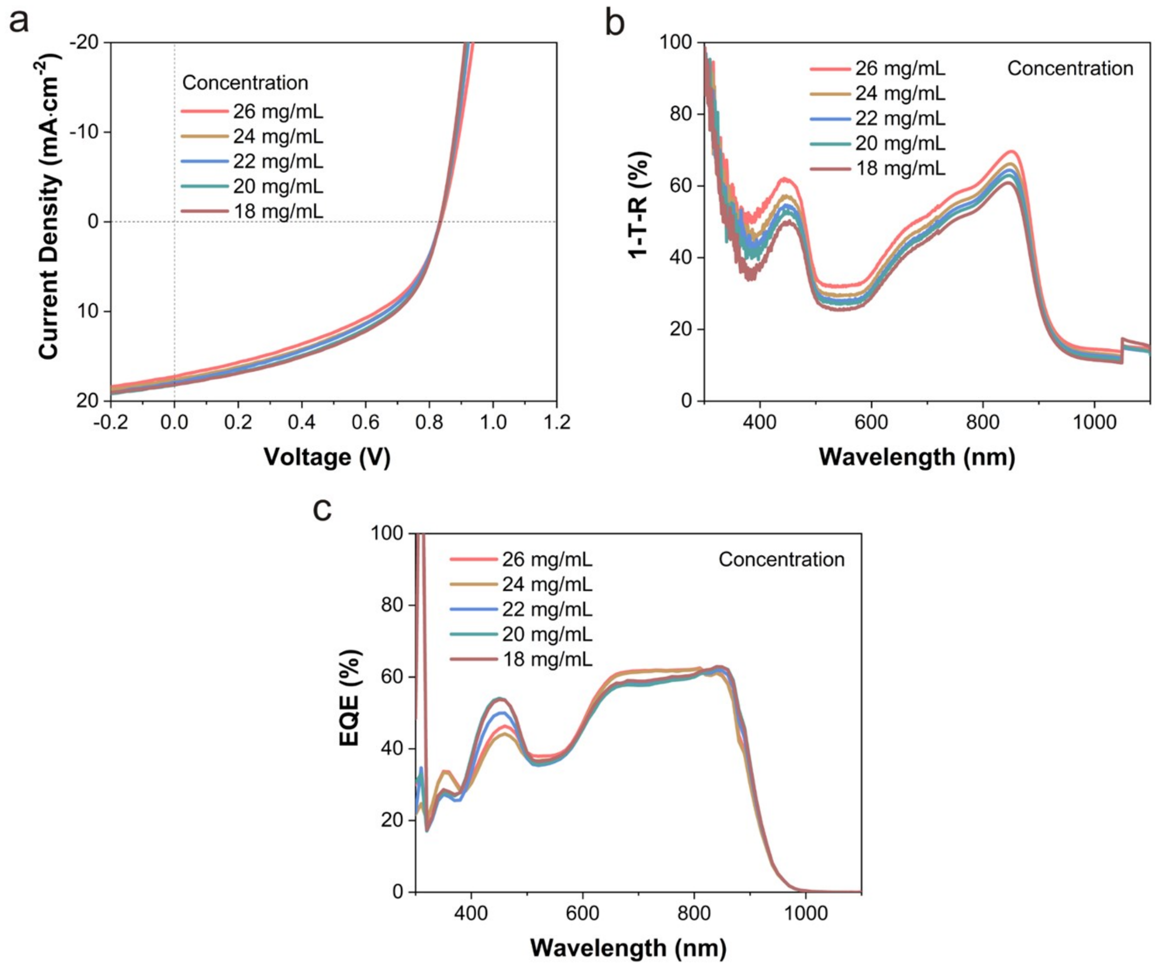

Figure S12. *J-V* (a), 1-T-R (b) and EQE (c) curves of devices with different total concentrations for active layers.

Table S8. Device performances with different total concentrations for active layers.

Concentration	V_{OC} (V)	J_{SC} / J_{EQE} (mA·cm^{-2})	FF (%)	PCE (%)
26 mg/mL	0.834	17.2/17.6	44.8	6.43
24 mg/mL	0.833	17.6/17.4	46.2	6.77
22 mg/mL	0.832	17.9/17.4	45.9	6.83
20 mg/mL	0.833	18.1/17.6	47.5	7.17
18 mg/mL	0.832	18.1/17.7	48.6	7.32

Table S9. Device performances with different donors.

Donor	V_{OC} (V)	J_{SC} / J_{EQE} (mA·cm^{-2})	FF (%)	PCE (%)
TPD-2TPA	0.833	18.7/18.5	47.2	7.34
TPD-2TPA-4Me	0.779	11.6/11.0	48.6	4.40
TPD-2TPA-4Bu	0.765	16.8/15.2	45.4	5.83
TPD-2TPA-4F	0.843	1.91/1.47	27.0	0.435

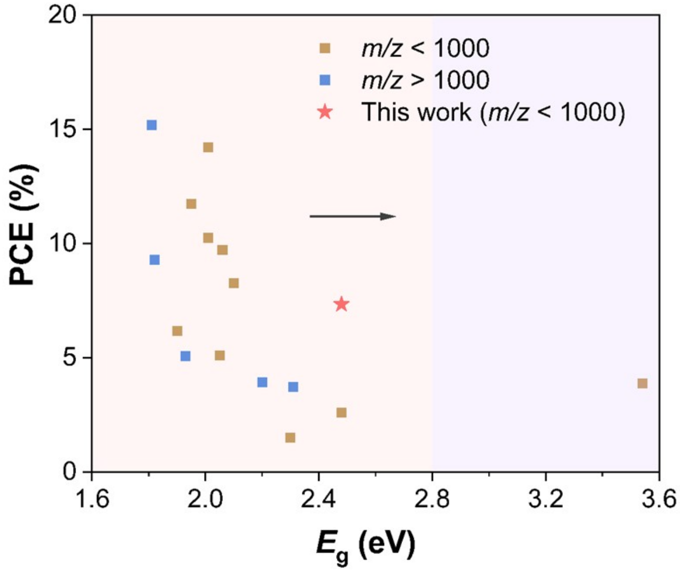

Figure S13. Performance statistics of small molecule donors with E_g over 1.80 eV in binary organic solar cells.

Table S10. Performance data statistics of small molecule donors with E_g over 1.80 eV in binary organic solar cells.

m/z of donor	No.	Donor	Acceptor	PCE (%)	E_g of donor (eV)	*m/z* of donor	Year
m/z > 1000	1[1]	TT-TTPA	$PC_{71}BM$	3.73	2.31	1128.0	2012
	2[2]	TPA(BT–3Cz)$_3$	$PC_{71}BM$	3.94	2.20	1478.2	2015
	3[2]	TPA(BT–T–3Cz)$_3$	$PC_{71}BM$	5.07	1.93	1724.2	2015
	4[3]	BTR	$PC_{71}BM$	9.30	1.82	2027.7	2015
	5[4]	B3T-P	BO-4Cl	15.2	1.81	1857.1	2021
m/z < 1000	6[5]	D	A2 (12Cl-cHBC)	1.50	2.30	761.2	2017
	7[6]	TPD-2TPA	$PC_{71}BM$	2.60	2.48	751.3	2017
	8[7]	TAPC	Y6	3.88	3.54	626.9	2021
	9[8]	TPA-T-DCV-Ph	C_{70}	5.11	2.05	479.1	2018
	10[9]	M2	$PC_{71}BM$	6.18	1.90	630.3	2018
	11[10]	C1	BThIND-Cl	8.26	2.10	390.5	2021
	12[10]	C2	Y6	9.72	2.06	514.6	2021
	13[11]	C1-CN	DBTBT-IC	10.3	2.01	438.2	2022
	14[11]	C2-CN	DBTBT-IC	11.7	1.95	562.2	2022
	15[12]	C1-CN	F13	14.2	2.01	438.2	2023
	16	TPD-2TPA	Y6	7.34	2.48	751.3	This work

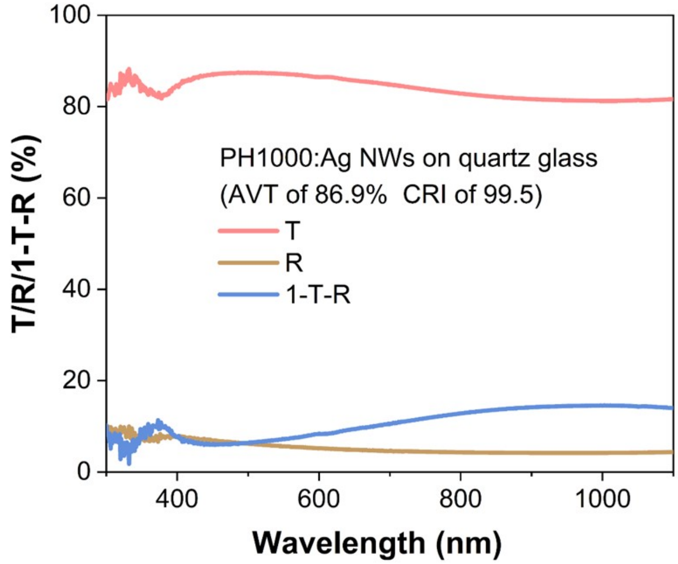

Figure S14. T/R spectra of the transparent electrode on quartz glass.

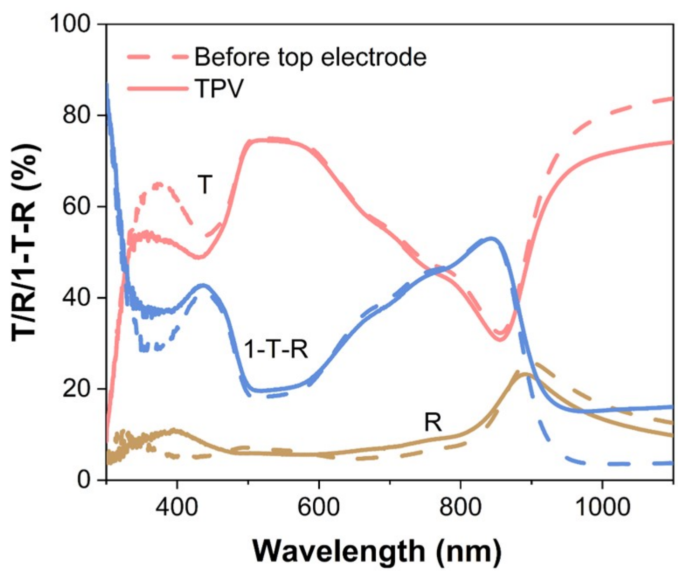

Figure S15. T/R spectra of the device before and after the top electrode with TPV AVT of 71.5%.

Table S11. Device performances with various SVA durations or thermal annealing for active layers (TPV AVT~70%).

SVA	Anneal	V_{OC} (V)	J_{SC} (mA·cm^{-2})	FF (%)	PCE (%)
0 s	R.T.	0.856	7.88	36.7	2.48
10 s	R.T.	0.825	10.7	41.8	3.69
30 s	R.T.	0.823	15.0	46.5	5.75
40 s	R.T.	0.804	16.1	46.8	6.05
1 min	R.T.	0.804	15.6	47.7	5.99
2 min	R.T.	0.798	16.2	45.2	5.83
0 s	140 °C	0.828	15.8	47.9	6.26

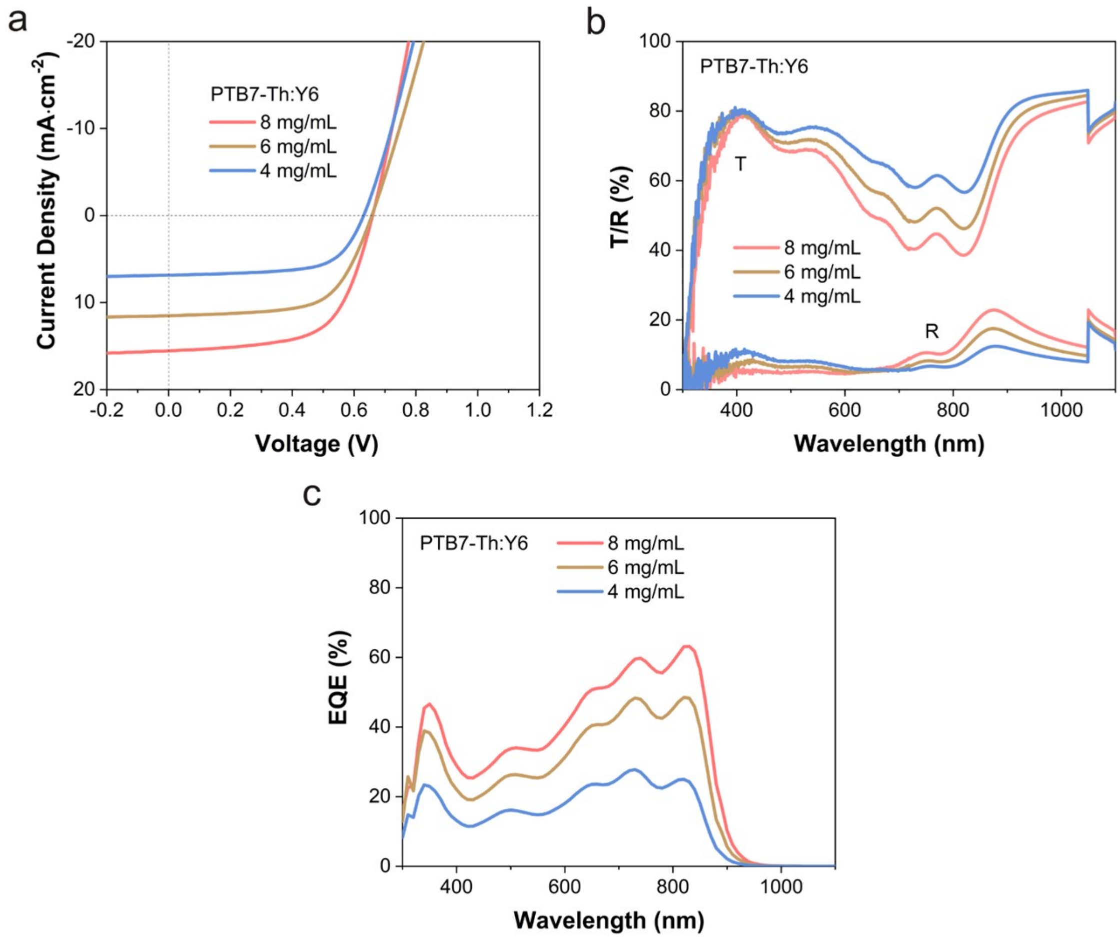

Figure S16. PTB7-Th:Y6-based opaque device performances. *J-V* curves of devices (a), T/R spectra of related films (b) and EQE curves of devices (c) with different total concentrations for active layers.

Table S12. PTB7-Th:Y6-based opaque device performances with different total concentrations for active layers.

Concentration	V_{OC} (V)	J_{SC} (mA·cm^{-2})	FF (%)	PCE (%)	AVT of Film (%)	CRI of Film
8 mg/mL	0.660	15.5/14.9	62.4	6.39	64.8	86.4
6 mg/mL	0.657	11.5/11.5	63.5	4.80	68.8	90.4
4 mg/mL	0.631	6.85/6.40	65.0	2.81	73.4	94.5

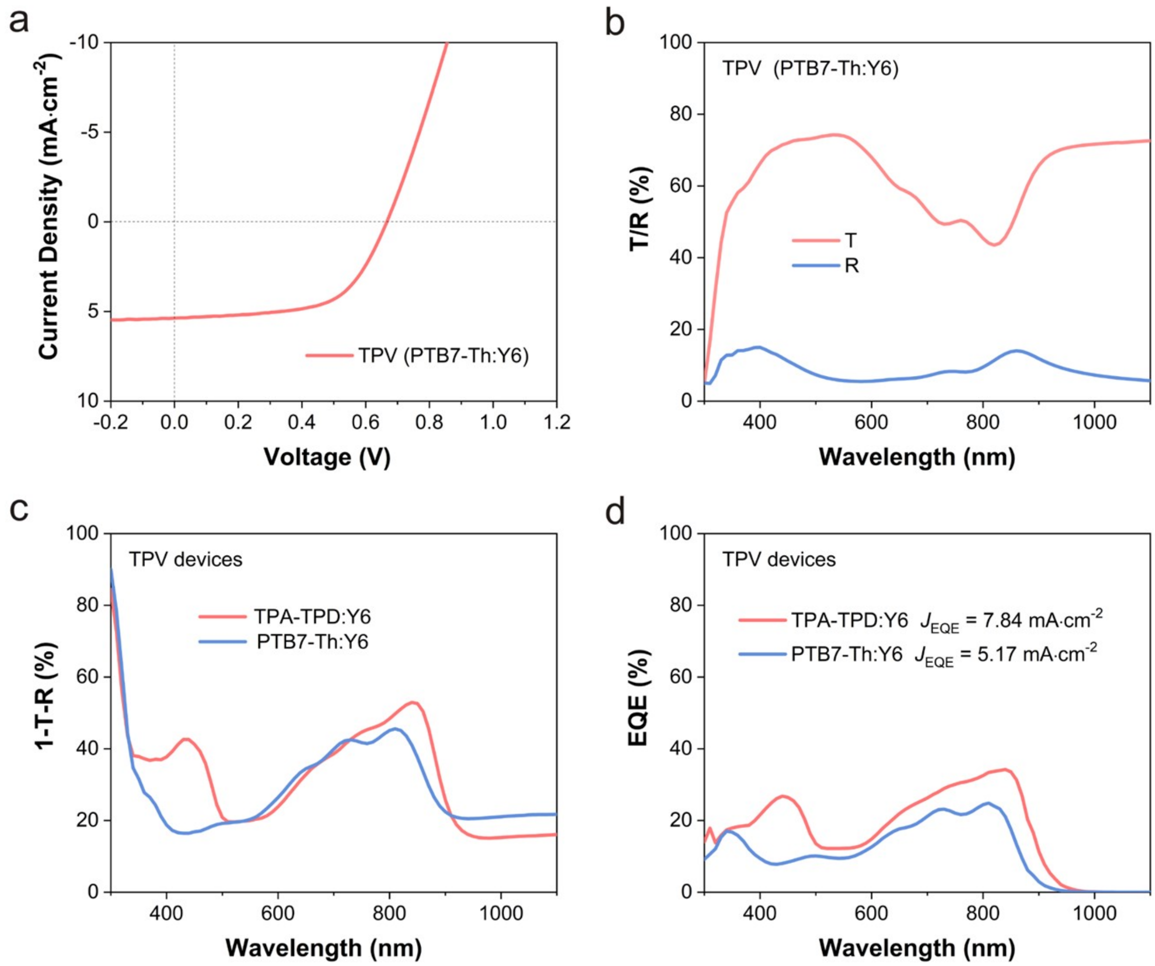

Figure S17. *J-V* curve (a) and T/R spectra (b) for PTB7-Th:Y6-based TPV device with AVT of 71.1%. 1-T-R (c) and EQE (d) curves for the TPD-2TPA:Y6-based and PTB7-Th:Y6-based TPV device with AVT ~ 71%.

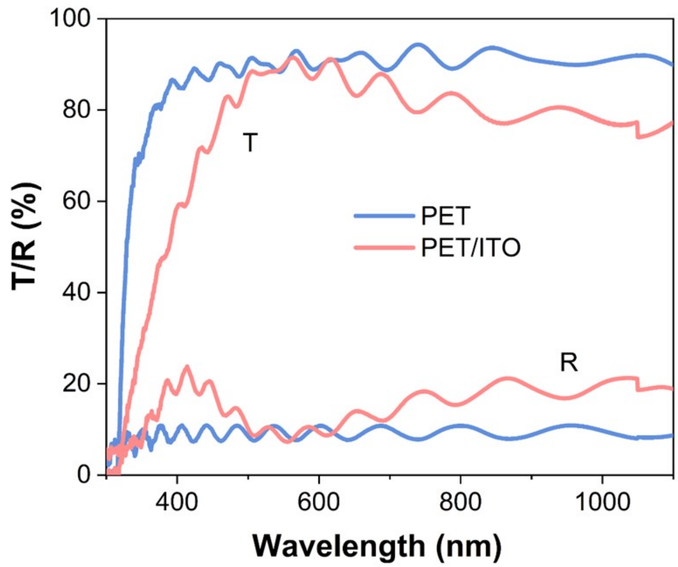

Figure S18. T/R properties for the flexible substrates.

Table S13. AVT and CRI values for the flexible substrates.

Substrate	AVT (%)	CRI
PET	90.3	98.6
PET/ITO	88.4	97.4

Table S14. Flexible opaque device performances with various SVA durations at room temperature (14 mg/mL).

SVA	V_{OC} (V)	J_{SC} (mA·cm^{-2})	FF (%)	PCE (%)
0 s	0.838	9.25	36.4	2.83
10 s	0.827	11.0	38.9	3.55
30 s	0.784	17.9	37.3	5.25
40 s	0.755	16.9	36.2	4.62
1 min	0.759	14.7	39.8	4.44
2 min	0.0605	0.564	24.7	0.0084

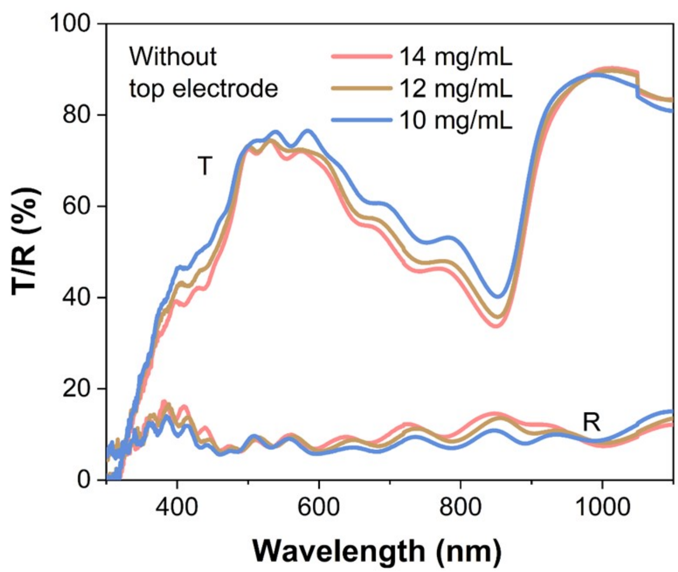

Figure S19. T/R spectra of the flexible samples before transferring the top electrodes with different concentrations for active layers.

Table S15. AVT and CRI values of the flexible samples before and after transferring the top electrodes with different concentrations for active layers.

Concentration	Condition	AVT (%)	CRI
14 mg/mL	Before top electrode	69.5	91.2
	TPV device	66.8	89.3
12 mg/mL	Before top electrode	70.7	92.4
	TPV device	68.3	90.0
10 mg/mL	Before top electrode	73.1	93.7
	TPV device	70.6	91.2

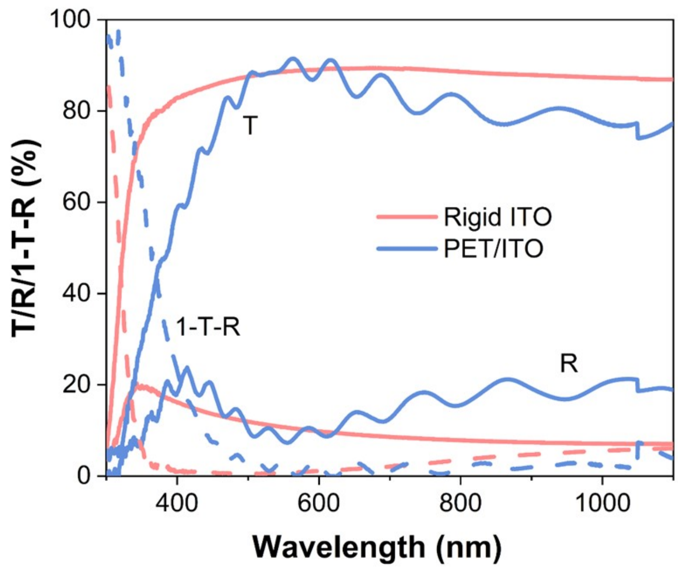

Figure S20. T/R/1-T-R spectra of the rigid ITO and flexible ITO substrates.

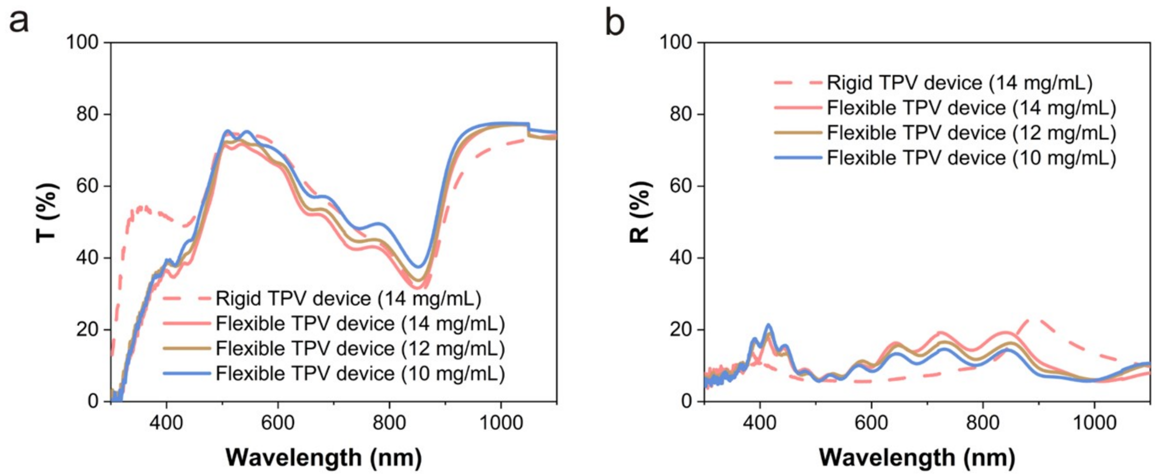

Figure S21. T (a) and R (b) spectra of the rigid TPV device and flexible TPV devices.

Table S16. Flexible TPV device performances with TPV AVT of 70.6%.

Device	V_{OC} (V)	J_{SC} /J_{EQE} (mA·cm^{-2})	FF (%)	PCE (%)
Flexible TPV	0.828	6.94/6.93	41.6	2.39

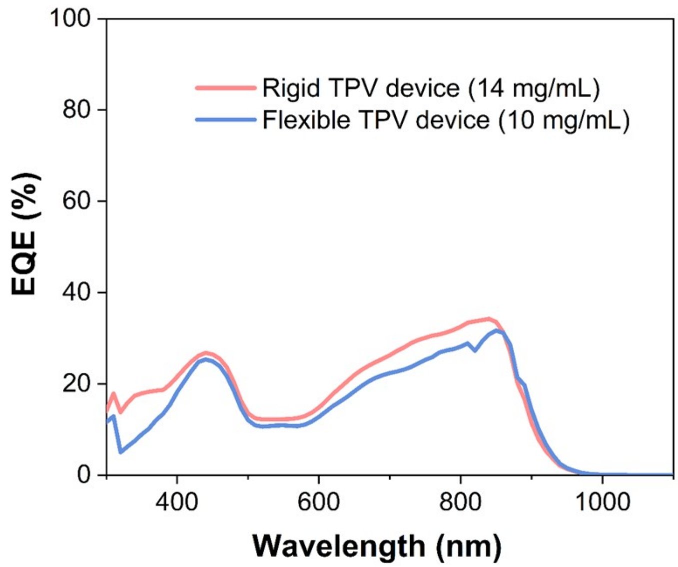

Figure S22. EQE curves of the rigid and flexible TPV device with TPV AVT around 70%.

Table S17. Performance data statistics of donors with E_g over 2.20 eV in binary organic solar cells.

No.	Donor	Acceptor	PCE (%)	E_g of donor (eV)	*m/z* of donor	Year
1[5]	D	A2 (12Cl-cHBC)	1.50	2.30	761.2	2017
2[13]	PTAA	Y6	2.29	2.95	/	2022
3[6]	TPD-2TPA	$PC_{71}BM$	2.60	2.48	751.3	2017
4[7]	TAPC	Y6	3.88	3.54	626.9	2021
5[2]	TPA(BT–3Cz)$_3$	$PC_{71}BM$	3.94	2.20	1478.2	2015
6[13]	PF8TAA	Y6	4.76	2.87	/	2022
7[13]	PF8TAA-C6	Y6	5.56	2.87	/	2022
8[13]	PF8TAA-C12	Y6	6.07	2.87	/	2022
9	TPD-2TPA	Y6	7.34	2.48	751.3	This work

REFERENCES

1. Q. Shi, P. Cheng, Y. Li and X. Zhan, *Adv. Energy Mater.*, 2012, **2**, 63-67.

2. P. Zhou, D. Dang, Q. Wang, X. Duan, M. Xiao, Q. Tao, H. Tan, R. Yang and W. Zhu, *J. Mater. Chem. A*, 2015, **3**, 13568-13576.

3. K. Sun, Z. Xiao, S. Lu, W. Zajaczkowski, W. Pisula, E. Hanssen, J. M. White, R. M. Williamson, J. Subbiah, J. Ouyang, A. B. Holmes, W. W. Wong and D. J. Jones, *Nat. Commun.*, 2015, **6**, 6013.

4. C. An, Y. Qin, T. Zhang, Q. Lv, J. Qin, S. Zhang, C. He, H. Ade and J. Hou, *J. Mater. Chem. A*, 2021, **9**, 13653-13660.

5. N. C. Davy, M. Sezen-Edmonds, J. Gao, X. Lin, A. Liu, N. Yao, A. Kahn and Y.-L. Loo, *Nat. Energy*, 2017, **2**, 17104.

6. C. Garcias-Morales, D. Romero-Borja, J. L. Maldonado, A. E. Roa, M. Rodriguez, J. P. Garcia-Merinos and A. Ariza-Castolo, *Molecules*, 2017, **22**, 1607.

7. H. Tang, J. Wu, H. Liu, B. Wang, H. Wang, Y. Li, Y. Fu and Z. Xie, *Organic Electronics*, 2021, **93**, 106140.

8. O. V. Kozlov, Y. N. Luponosov, A. N. Solodukhin, B. Flament, O. Douhéret, P. Viville, D. Beljonne, R. Lazzaroni, J. Cornil, S. A. Ponomarenko and M. S. Pshenichnikov, *Org. Electron.*, 2018, **53**, 185-190.

9. S. Revoju, S. Biswas, B. Eliasson and G. D. Sharma, *Phys. Chem. Chem. Phys.*, 2018, **20**, 6390-6400.

10. R. Pradhan, H. Dahiya, B. P. Bag, M. L. Keshtov, R. Singhal, G. D. Sharma and A. Mishra, *J. Mater. Chem. A*, 2021, **9**, 1563-1573.

11. R. Pradhan, A. Agrawal, B. P. Bag, R. Singhal, G. D. Sharma and A. Mishra, *ACS Appl. Energy Mater.*, 2022, **5**, 9020-9030.

12. G. D. Sharma, R. Pradhan, K. Khandelwal, R. Singhal, W. Liu, X. Zhu and A. Mishra, *J. Mater. Chem. C*, 2023, **11**, 1919-1926.

13. Z. Du, Q. Xue, K. Zhang, Z. Hu, Z. Zhou, J. Jing, L. Shao, N. Li and F. Huang, *Solar RRL*, 2022, **6**, 2200527.